THE FASEB JOURNAL • RESEARCH • www.fasebj.org

Apelin impairs myogenic response to induce diabetic nephropathy in mice

Jia Zhang,*,[1,2] Jiming Yin,†,[1] Yangjia Wang,*,[2] Bin Li,*,[2] and Xiangjun Zeng*,[2,3]
*Department of Pathophysiology and †Beijing Institute of Hepatology, Beijing You An Hospital, Capital Medical University, Beijing, China

ABSTRACT: The cause of the invalid reaction of smooth muscle cells to mechanical stimulation that results in a dysfunctional myogenic response that mediates the disruption of renal blood flow (RBF) in patients with diabetes is debatable. The present study revealed that increased apelin concentration in serum of diabetic mice neutralized the myogenic response mediated by apelin receptor (APJ) and resulted in increased RBF, which promoted the progression of diabetic nephropathy. The results showed that apelin concentration, RBF, and albuminuria:creatinine ratio were all increased in kkAy mice, and increased RBF correlated positively with serum apelin both in C57 and diabetic mice. The increased RBF was accompanied by decreased phosphorylation of myosin light chain (MLC), β-arrestin, and increased endothelial NOS in glomeruli. Meanwhile, calcium, phosphorylation of MLC, and β-arrestin were decreased by high glucose and apelin treatment in cultured smooth muscle cells, as well. eNOS was increased by high glucose and increased by apelin in cultured endothelial cells (ECs). Knockdown of β-arrestin expression in smooth muscle cells cancelled phosphorylation of MLC induced by apelin. Therefore, apelin may induce the progression of diabetic nephropathy by counteracting the myogenic response in smooth muscle cells.—Zhang, J., Yin, J., Wang, Y., Li, B., Zeng, X. Apelin impairs myogenic response to induce diabetic nephropathy in mice. FASEB J. 32, 000–000 (2018). www.fasebj.org

KEY WORDS: smooth muscle cell · renal blood flow · endothelial cell · APJ · kidney

The myogenic response is an important mechanism in controlling renal blood flow (RBF) (1–3), and its dysfunction in type 2 diabetes correlates positively with microalbuminuria (2, 4, 5). Different GPCRs have been reported to mediate myogenic tone by working as mechanoreceptors (6, 7). APJ, a GPCR expressed in vascular smooth muscle cells (VSMCs) and endothelial cells (ECs) (8), has been reported to mediate endothelium-dependent vasodilation (9) and is down-regulated in blood vessels in type 2 diabetes (10). Recently, apelin, an endogenous ligand of APJ, was reported to inhibit APJ-mediated cardiac hypertrophy in a transverse aortic constriction model (11) and to contribute microalbuminuria in diabetic nephropathy (DN) in patients with type 2 diabetes and in mice (3). Therefore, it is hypothesized that increased apelin associated with obesity in type 2 diabetes aggravates the impaired myogenic response induced by high glucose, which results in imbalanced perfusion in kidney and microalbuminuria in DN.

As disruption of the endothelium did not impair the pressure-induced myogenic vasoconstriction (2), it is now assumed that myogenic responsiveness is an inherent property of VSMCs that can be fine tuned by endothelial and neuronal or hormonal factors (12, 13), through action on mechanosensors, such as GPCRs (14). Then, is apelin involved in the impairment of myogenic tone in DN? It has been reported that apelin depressed stretch-induced cardiac hypertrophy by combining with APJ in cardiomyocytes (11), and it is hypothesized that apelin suppresses blood pressure–induced VSMC contraction by binding with APJ. The underlying signaling pathways of mechanosensors in VSMCs are reported to be phosphorylated myosin light chain (pMLC), phosphorylated myosin light chain kinase (pMLCK), Ca^{2+} contents, and corresponding factors activated by stimulated receptors (2, 6, 9). The purpose of the present study was to understand the actions and signaling pathways of apelin on VSMCs and ECs, which impair the myogenic tone and result in uncontrolled RBF in DN.

The animals used as a model for DN are kkAy mice. The kkAy mouse model is considered to be similar to human type 2 diabetes (15). The animals exhibit obesity, glucose

ABBREVIATIONS: ACR, albumin:creatinine ratio; APJ, anti-putative receptor protein related to the angiotensin receptor AT1; DBP, diastolic blood pressure; DN, diabetic nephropathy; EC, endothelial cell; FBS, fetal bovine serum; HEPES, 4-(2-hydroxyethyl)-1-piperazineethanesulfonic acid; L-NAME, N^G-nitro-L-arginine methyl ester, hydrochloride; MLC, myosin light chain; MLCK, myosin light chain kinase; pMLC, phosphorylated myosin light chain; pMLCK, phosphorylated myosin light chain kinase; RBF, renal blood flow; SBP, systolic blood pressure; VSMC, vascular smooth muscle cell

[1] These authors contributed equally to this work.
[2] Current affiliation: Department of Pathophysiology, Capital Medical University, Beijing, China.
[3] Correspondence: Capital Medical University, You Anmen Wai No. 10, Beijing 100069, China. E-mail: megan_zeng@163.com

doi: 10.1096/fj.201701257R

intolerance, insulin resistance, dyslipidemia, and hypertension. The kkAy mice also develop renal disease characterized by moderate albuminuria with mild glomerular disease and podocyte loss (15, 16).

MATERIALS AND METHODS

Experimental animals

All animal studies were conducted according to The Animal Care and Use Committee of Capital Medical University (20100610). All animals received humane care, and the experimental protocol was approved by the Committee of Laboratory Animals according to institutional guidelines.

Eight-week-old male kkAy mice and control C57BL/6J (C57) mice were purchased from Capital Medical University (Beijing, China). Mice were housed in air-conditioned, specific pathogen-free animal quarters with lighting from 8 AM to 9 PM and were given unrestricted access to standard laboratory water throughout the study. Animals were fed on semipurified moderately high-fat diet containing 24% kcal fat and 0.2% cholesterol.

The mice were then randomly divided into saline groups (C57+saline and kkAy+saline groups; both $n = 12$), which were intraperitoneally injected with vehicle, using an Alzet micro-osmotic pump (model 1004; Durect, Cupertino, CA, USA); apelin treatment groups (C57+apelin and kkAy+apelin groups; both $n = 12$), which were intraperitoneally injected with apelin-13 (A6469, 30 μg/kg/d; MilliporeSigma, Billerica, MA, USA) for 4 wk, using the Alzet pump; and an F13A treatment group (C57+F13A group, $n = 12$; kkAy+F13A, $n = 12$), which was intraperitoneally injected with F13A, the antagonist of apelin-13,057-29 (25 μg/kg/d; Phoenix Pharmaceuticals, Strasbourg, France) for 4 wk, using the Alzet pump. The body weight was measured in unfed mice at the end of the experiments. The urine sample was collected for 24 h from each mouse housed in a metabolic cage (Tecniplast, Buguggiate, Italy). Albumin and creatinine were detected immediately after the sample was collected. The mice were euthanized after the 8 wk treatments, at 12 wk of age.

Biochemical characterization

Twenty-four-hour urine samples were used for detection of urinary albumin (CSB-E13437m; Cusabio Biotech Co. Wuhan, China) and creatinine (CSB-E12745m; Cusabio Biotech Co.) with ELISA kits. All analyses were performed in accordance with the manufacturer's instructions. The urinary albumin:creatinine ratio (ACR) = urinary albumin (μg)/urinary creatinine (mg).

Apelin concentrations were measured with a Radioimmunoassay Kit (Phoenix Pharmaceuticals), according to the manufacturer's instructions, in serum collected from euthanized mice and stored in −80°C until use.

Perfusion of isolated kidneys

Perfusion of mouse isolated kidneys was performed according a previously published method (17). In brief, the mice were anesthetized with 2,2,2-tribromoethanol (10 μl/g of body weight; T48402-5G; MilliporeSigma). The aorta and vena cava were exposed by removing the intestine to the left side of the mouse lateral from the abdomen. The left kidney was dissected from the connective tissue after the aorta was cannulated with a needle. For perfusion, the isolated kidney was connected to a rotary pump that was filled with perfusate, containing 1 mM $CaCl_2$, 140 mM NaCl, 6 mM KCl, 1 mM $MgSO_4$, 5 mM glucose, 10 mM 4-(2-hydroxyethyl)-1-piperazineethanesulfonic acid) (HEPES), 95% O_2, and 5% CO_2, and controlled by the Panlab system (ML176-220; ADInstruments, Shanghai, China). The perfusion pressure was increased step by step with the rotary pump from 30 to 190 mmHg at 30 mmHg per minute intervals. The volume of perfusate out of the renal vein was measured for each perfusion pressure. Kidneys from C57 mice and kkAy mice were isolated and perfused with apelin, F13A, or apelin and L-NAME (s0006; Beyotime, Beijing, China). The experiments were repeated 6 times in every group.

Systolic blood pressure measurement

Systolic blood pressure (SBP) and diastolic blood pressure (DBP) were measured with the tail-cuff system (softtron BP-98A; Softron, Tokyo, Japan) and the telemetric blood pressure system (TA-PA11C10; Data Sciences International, Tilburg, The Netherlands) in conscious mice (18). Measurements were taken on 3 different days at 3 different settings, averaging at least 6 readings.

Doppler measurement of renal blood velocity

Peak systolic renal artery blood velocity and the diameter of the artery were measured with the Vevo2100 imaging system (PW mode; VisualSonics, Toronto, ON, Canada). After a brief stabilization period, pulsed-wave Doppler blood velocity and diameter of the artery were obtained in the renal artery before it enters the kidney to provide a measure of renal blood velocity and diameter of the artery. Total RBF was calculated with velocity multiplied by diameter.

Immunohistochemistry

Three tissue sections at 4 μm (no. 1, 6, and 12) in each group were used to perform immunostaining for β-arrestin-2 with mouse anti-β-arrestin-2 antibody (sc-13140; Santa Cruz Biotechnology, Dallas, TX, USA). The secondary antibody was donkey anti-mouse-horseradish peroxidase. Color was developed by incubating with diaminobenzidine and counterstaining with hematoxylin. Images were obtained with a BX63 Upright Microscope (Olympus, Tokyo, Japan).

Cell culture

VSMCs were isolated by autogrowth of explant culture from the renal artery of mice, as previously described (19). In brief, mouse thoracic aortas were removed and washed with DMEM. The intima and inner two-thirds of the medium was carefully dissected from the vessels and cut into pieces (1 mm^2). The tissue pieces were then explanted onto a 0.02% gelatin-coated flask and cultured in DMEM supplemented with 20% fetal bovine serum (FBS), 100 U/ml penicillin, and 100 g/ml streptomycin. The cells were allowed to autogrow for 2 wk, passaged, and maintained in DMEM supplemented with 10% FBS, 100 U/ml penicillin, and 100 g/ml streptomycin. Cells were cultured at 37°C in a humidified atmosphere with 5% CO_2.

Endothelial cells were isolated from glomeruli in renal cortices of adult male C57BL/6 mice (3). In brief, the cortex slices were mashed by differential sieving, which were 100, 76, and 54 μm in size; the tissues left on the mesh sieve with 54 μm in size were glomeruli. The isolated glomeruli were digested with 0.1% collagenase type IV (Millipore Sigma) for 15 min. The cell suspension was cultured in M199 medium (Thermo Fisher Scientific) supplemented with 20% FBS (HyClone Laboratories, Logan, UT, USA), 100 U/ml penicillin, 100 g/ml streptomycin, and 75 μg/ml

endothelial cell growth supplement (ECGS; MilliporeSigma), on 1% gelatin-coated (MilliporeSigma) 25-cm^2 flasks in a humidified incubator at 37°C under 5% CO_2. The cultured cells were identified by morphologic observation and positive staining with antibodies raised against von Willebrand factor. The third to fifth passages of the glomerular endothelial cells were used in subsequent experiments.

β-Arrestin knockdown in VSMCs

To knock down β-arrestin-1 in VSMCs, cells were cotransfected with β-arrestin-1 CRISPR/Cas9 KO Plasmid (sc-430955-KO-2) and β-arrestin-1 HDR plasmid (sc-430955-HDR-2; both from Santa Cruz Biotechnology), with Lipofectamine 2000 transfection reagent used as described by the manufacturer (Thermo Fisher Scientific). To knock down β-Arrestin-2 in VSMCs, cells were cotransfected with β-arrestin-2 CRISPR/Cas9 KO Plasmid (sc-432139) and β-arresin-2HDR Plasmid (sc-432139-HDR; both from Santa Cruz Biotechnology), using Lipofectamine 2000 Transfection Reagent, as described by the manufacturer. After transfection, the cells were immediately used for the following experiments. The expression of β-arrestin was detected by Western blot analysis.

Stretch induction

Hypotonic stretching (in HEPES buffers) was used in smooth muscle cells (11). HEPES buffers for stretching experiments contained 65 mM NaCl, 10 mM HEPES, 4.2 mM KCl, 0.5 mM $MgCl_2$, 1 mM $CaCl_2$, and 5.5 mM glucose, with the addition of 10 mM (hypotonic) or 160 mM (isotonic) mannitol (pH 7.4). The osmolality of the hypotonic HEPES buffer was 160 mosmol/kg water, and that of the isosmotic buffer was 332 mosmol/kg water.

Mechanical stretch was provided by the FX-4000T Strain Unit (Flexcell International, Burlington, NC, USA) (20). Cells were seeded on flexible silicone-bottom plates (Flexcell International) at a density of 3×10^5 cells per well. Twenty-four hours later, the culture medium was replaced with serum-free medium for another 24 h to synchronize the cells. Cells in the serum-free medium were then exposed to cyclic stretching with an elongation magnitude of either 5 or 15%, at a consistent frequency of 1.25 Hz, with or without apelin (1.0 nM) or F13A (1.0 nM).

Calcium measurement in VSMCs

Fluorescence confocal microscopy (LSM5 Pascal Laser Scanning Confocal Microscope; Zeiss, Jena, Germany) and the Ca^{2+} dye Fluo-4 AM were used to detect calcium concentration changes in smooth muscle cells, as reported in Zeng *et al*. (21). In brief, VSMCs were preincubated for 30 min with Fluo-4 AM (f14201; Thermo Fisher Scientific), the medium was changed to fresh DMEM, and the cells were incubated for another 30 min. After hypotonic or isotonic buffer treatment, with or without apelin (1.0 nM) or F13A (1.0 nM) in the buffer, the Fluo-4 AM fluorescence intensity of similar populations of cells was detected for 20 min, and the fluorescence density was analyzed with software with the confocal microscope. The experiment was repeated 3 times.

Western blot analysis of protein expression

The proteins from tissues or cells were fractionated by electrophoresis on 10% SDS-PAGE, electroblotted to PVDF filter membranes, and incubated with the primary antibody at 4°C and then with a horseradish peroxidase–conjugated secondary antibody. The experiment was repeated 3 times. Primary antibodies were rabbit anti-APJ (sc-33823; Santa Cruz Biotechnology), rabbit anti-pMLC (3675; Cell Signaling Technology, Danvers, MA, USA), rabbit anti-MLC (3672; Cell Signaling Technology), goat anti-arrestin-1 (sc-9182; Santa Cruz Biotechnology), mouse anti-arrestin-2 (sc-13140; Santa Cruz Biotechnology), rabbit anti-eNOS (9572; Cell Signaling Technology), rabbit anti-p-eNOS (9570; Cell Signaling Technology), rabbit anti MLCK (ab76092; Abcam, Cambridge, MA, USA), and rabbit anti-p-MLCK (ab200809; Abcam). Densitometry was performed with ImageJ software (National Institutes of Health, Bethesda, MD, USA). To verify equal loading, antibody to glyceraldehyde 3-phosphate dehydrogenase was used.

Statistics

Data are summarized as means ± SD. A value of $P < 0.05$ was considered significant. All reported significance values are 2-tailed. Analyses were performed with SPSS v13.0 for the PC (IBM, Armonk, NY, USA). Differences between groups were evaluated for significance with independent Student's *t* test or 1-way ANOVA and Newman-Keuls *post hoc* tests.

RESULTS

Body weight, blood glucose, and blood pressure

Apelin and F13A (the antagonist of apelin) had no effect on body weight in both C57 and kkAy mice (**Table 1**). kkAy mice had higher body weights compared to C57 mice at both 8 and 12 wk of age. kkAy mice were hyperglycemic compared with C57 mice at both 8 and 12 wk of age. Apelin and F13A (the antagonist of apelin) treatment had

TABLE 1. *Body weight and fasting blood glucose in both groups*

Group		Fasting blood glucose (mM)		Body weight (g)	
Mouse	Treatment	8 wk old	12 wk old	8 wk old	12 wk old
C57	Saline	5.4 ± 0.5	5.5 ± 0.6	28.6 ± 2.7	31.3 ± 4.1
	Apelin	5.5 ± 0.6	5.6 ± 0.5	27.9 ± 2.0	28.3 ± 1.5
	F13A	5.4 ± 0.4	5.5 ± 0.6	28.0 ± 1.7	26.3 ± 1.2
kkAy	Saline	8.9 ± 0.7*	11.3 ± 1.2*	38.5 ± 2.3*	35.3 ± 2.9*
	Apelin	9.0 ± 0.8*	13.8 ± 2.1*	39.1 ± 3.0*	37.2 ± 4.2*
	F13A	9.0 ± 0.8*	9.8 ± 1.9*	38.4 ± 4.1*	38.3 ± 3.9*

Data are means ± SD ($n = 12$/group). *$P < 0.05$ compared to C57 mice with the same treatment.

TABLE 2. *Blood pressure changes in every group*

Group		8 wk old			12 wk old		
Mouse	Treatment	SBP (mmHg)	DBP (mmHg)	MBP (mmHg)	SBP (mmHg)	DBP (mmHg)	MBP (mmHg)
C57	Saline	106.2 ± 5.6	68.0 ± 3.1	80.8 ± 3.7	111.0 ± 4.7	78.2 ± 3.3	89.2 ± 4.2
	Apelin	107.3 ± 6.3	71.5 ± 3.2	83.5 ± 3.1	106.0 ± 4.3	67.8 ± 2.5	80.5 ± 3.6
	F13A	108.2 ± 5.4	68.7 ± 2.9	80.7 ± 4.2	105.7 ± 4.8	58.6 ± 3.1	74.4 ± 3.3
kkAy	Saline	125.7 ± 4.7*	91.7 ± 4.1*	103.2 ± 4.2*	134.0 ± 5.2*	98.3 ± 4.3*	110.3 ± 5.1*
	Apelin	126.2 ± 7.1*	95.1 ± 3.6*	105.4 ± 3.8*	124.3 ± 3.9*,†	81.8 ± 3.9*,†	96.1 ± 4.7*,†
	F13A	123.6 ± 5.8*	93.3 ± 4.6*	103.2 ± 4.5*	138.6 ± 4.9*	95.3 ± 4.9*	109.8 ± 5.8*

Data are means ± SD ($n = 12$/group). MBP, mean blood pressure. *$P < 0.05$ *vs.* C57 mice with the same treatment. †$P < 0.05$ *vs.* that in saline-treated kkAy mice.

no effect on blood glucose in both C57 mice and kkAy mice.

Mean blood pressure was higher in kkAy mice compared to C57 mice at both 8 and 12 wk of age. SBP and DBP followed the same pattern as mean arterial pressure (**Table 2**). Apelin significantly decreased blood pressure in kkAy mice, but no such effects were observed in C57 mice. F13A had no effect on blood pressure in C57 or kkAy mice.

Renal function and RBF

At 8 wk old, ACR in urine was higher in kkAy mice than that in C57 mice (**Fig. 1*A***); Renal blood flow was higher in

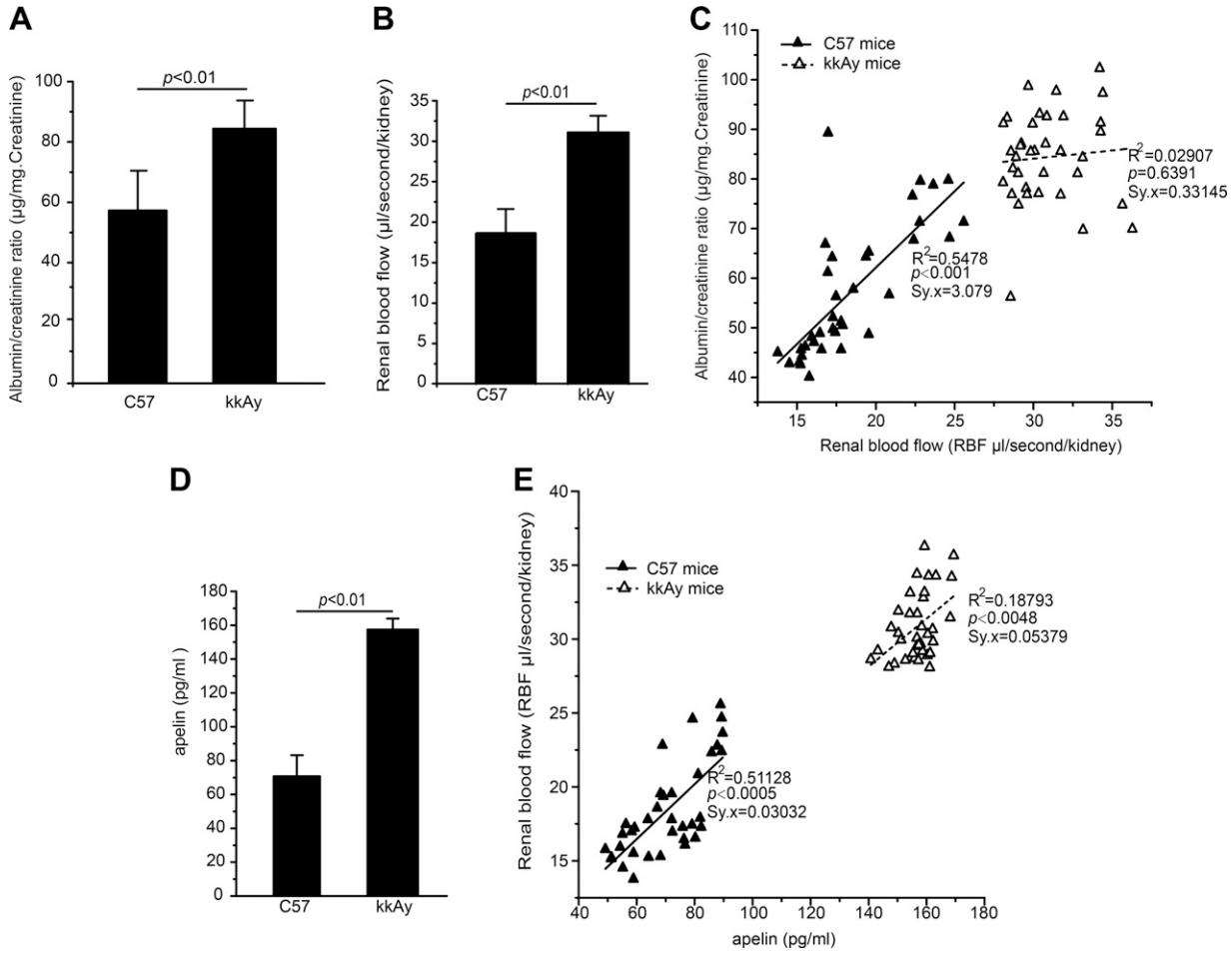

Figure 1. The correlation between serum apelin, RBF, and albuminuria in C57 and kkAy mice (n = 36 in both groups). *A*) Compared to C57 mice, the ACR increased significantly in kkAy mice (creatinine: 84.37 ± 9.36 μg/mg, kkAy *vs.* 57.26 ± 13.19 μg/mg, C57). *B*) RBF was significantly higher in kkAy mice (30.86 ± 2.28 μl/s per kidney) than in C57 mice (18.42 ± 3.21 μl/s per kidney). *C*) The ACR correlated positively with RBF in C57 and kkAy mice. *D*) Compared with C57 mice, serum apelin concentration was significantly higher in kkAy mice (kkAy, 156.76 ± 6.46 pg/ml mice *vs.* C57, 70.50 ± 3.21 pg/ml). *E*) RBF correlated positively with serum apelin concentration in both C57 and kkAy mice.

kkAy mice than in C57 mice (Fig. 1*B*). Accordingly, a correlation between ACR and RBF was observed in C57 and kkAy mice, and the slope of the regression line of kkAy mice was significantly different from that of control C57 mice (Fig. 1*C*).

Effects of apelin on RBF

Apelin has been reported to correlate with ACR in patients with DN (3), and we therefore measured the apelin concentration in serum. The results indicate that apelin concentration in serum was significantly increased in kkAy mice compared to C57 mice at 8 wk of age (Fig. 1*D*). Accordingly, a correlation between apelin concentration and RBF was observed in C57 and kkAy mice, and the RBF correlated positively with apelin concentration both in C57 and kkAy mice (Fig. 1*E*).

To investigate the effects of apelin on RBF and renal function, apelin and F13A (the antagonist of apelin) were used to treat 8-wk-old mice for 4 wk. RBF in the kkAy mice was significantly higher than that in the C57 mice at 12 wk of age. The 4-wk treatment with apelin significantly increased RBF and application of F13A reduced it (**Fig. 2*A, B***).

Besides increasing RBF, apelin treatment resulted in significantly increased ACR both in C57 and kkAy mice,

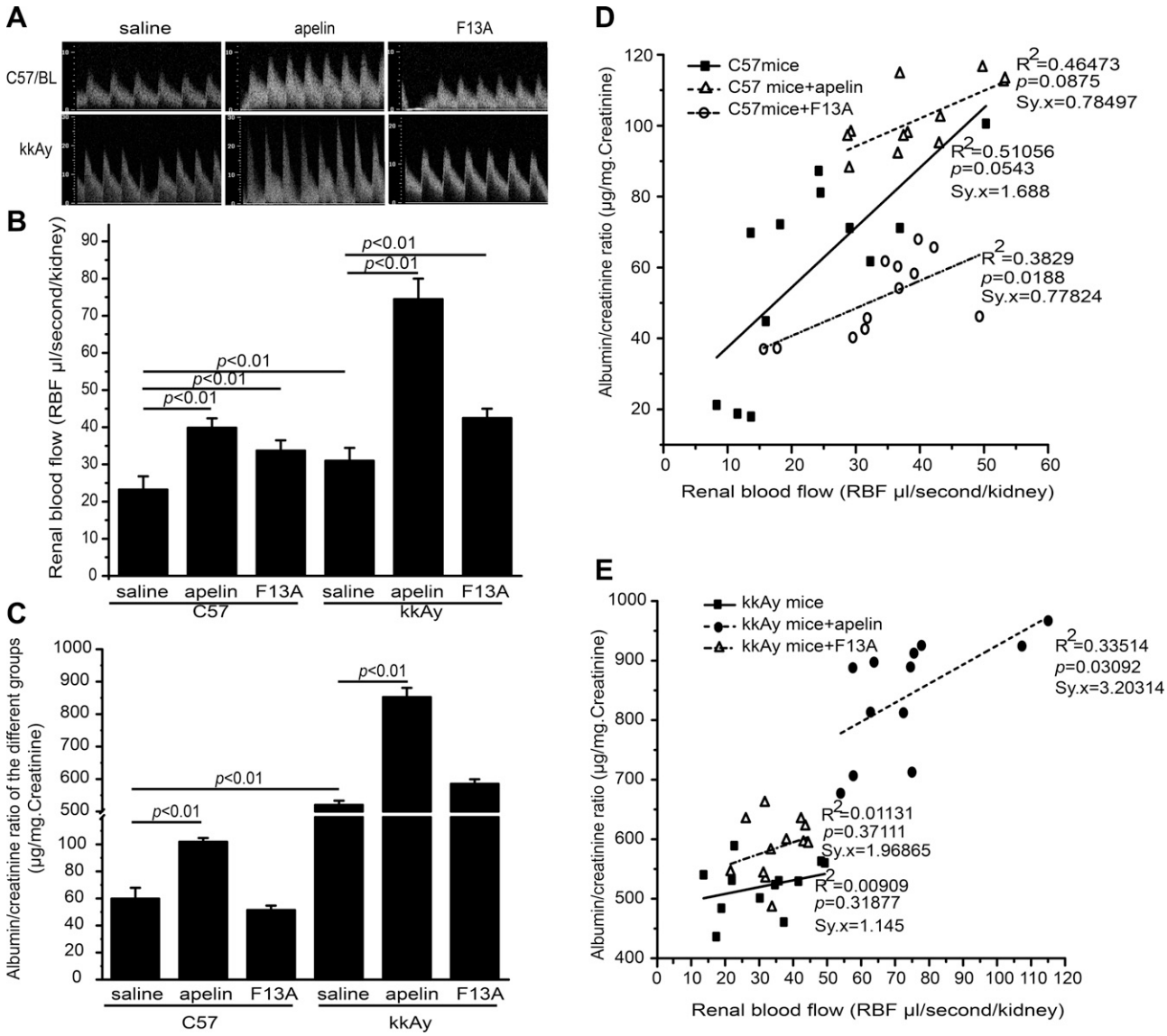

Figure 2. The effects of apelin on RBF and albuminuria in C57 mice and kkAy mice. *A*, *B*) The 4 wk treatment with apelin significantly increased the RBF in C57 mice (to 39.85 ± 2.55 µl/s per kidney) and kkAy mice (to 74.48 ± 5.49 µl/s per kidney). Four weeks with F13A reduced the RBF in kkAy mice (to 41.21 ± 1.89 µl/second per kidney) and C57 mice (35.08 ± 2.11 µl/s per kidney). RBF was significantly higher in kkAy mice (30.96 ± 3.48 µl/s per kidney) than in C57 mice (23.22 ± 3.54 µl/s per kidney) at 12 wk of age. *C*) Apelin significantly increased the ACR in C57 mice (to 101.89 ± 2.79 µg/mg creatinine) and kkAy mice (to 520.66 ± 12.67 µg/mg creatinine), whereas F13A did not show such effects (C57 mice, 51.38 ± 3.24 µg/mg creatinine *vs.* kkAy mice, 585.11 ± 14.63 µg/mg creatinine). *D*, *E*) Apelin and F13A decreased the slope of correlation between albuminuria and RBF in C57 mice. Apelin, but not F13A, significantly increased the slope of correlation between albuminuria and RBF in kkAy mice ($n = 12$).

whereas F13A significantly decreased ACR both in C57 and kkAy mice (Fig. 2*C*).

After apelin or F13A treatment for 4 wk, the mice still displayed significant correlation between RBF and ACR, but the slope of the regression line was significantly different between apelin- and F13A-treated C57 and kkAy mice (Fig. 2*D, E*).

Cell signaling pathways mediating apelin-induced vascular tone

As vascular contraction correlates with eNOS production in vascular endothelium and the phosphorylation state of 20 kDa MLC that drives myosin–actin interaction, the phosphorylation of MLC and eNOS were detected in renal artery and cortex of kidney. The results showed that pMLC was down-regulated in C57 and kkAy mice by apelin, whereas p-eNOS was up-regulated in both groups by apelin. On the other hand, F13A, the antagonist of apelin, increased the phosphorylation of MLC in C57 and kkAy mice (**Fig. 3**). These results suggest that apelin-induced vascular dilation is eNOS dependent, which is consistent with the published data (10).

As apelin has been reported to antagonize the mechanics of APJ in cardiomyocytes by activating β-arrestin (11), we sought to determine β-arrestin in renal artery and kidney cortex. The results showed that β-arrestin-1 and -2 were down-regulated in kkAy mice and further reduced by apelin, but increased by F13A (**Fig. 4**).These results suggest that apelin inhibits the mechanical sense in renal arterioles by reducing β-arrestin in kkAy mice.

Effects of apelin on isolated perfused kidney

To investigate direct effects of apelin on renal arterioles, isolated perfused kidneys were used to evaluate the pressure-induced change in blood flow. The results showed that the perfusion of kidneys isolated from kkAy mice was higher than in those from C57 mice at a perfusion pressure of 30–190 mmHg (**Fig. 5**). Apelin significantly increased the perfusion flow of isolated kidneys from both mouse groups. These effects were partially inhibited by L-NAME in kidneys from C57 mice, but not in those from kkAy mice. F13A increased the perfusion flow of isolated kidneys from both kkAy and C57 mice, even though the effect of F13A on increasing perfusion flow was less than the effect of apelin.

Effects of apelin on stretch-induced contraction of VSMCs

To demonstrate the direct effects of apelin on VSMCs in diabetic mice, we recorded the effects of apelin on phosphorylation of MLC and MLCK in VSMCs after stretch induction. The results showed that stretching increased phosphorylation of MLC in VSMCs (**Fig. 6*A, B***). Apelin decreased phosphorylation of MLC induced by stretching, whereas F13A (the antagonist of apelin) did not show such effects. Stretching decreased the phosphorylation of MLCK (Fig. 6*A, C*). Apelin increased phosphorylation of MLCK, and stretching inhibited it, whereas F13A, the antagonist of apelin, did not show any effects on it.

Calcium is important in the contraction of VSMCs; therefore, the effects of apelin on calcium were determined, before and after stretch induction. The results indicated that stretching induced an increase in calcium in VSMCs, whereas apelin and F13A inhibited the increase by 45 and 43% (**Fig. 7**). These results indicate that apelin may inhibit stretch-induced contraction of VSMCs by reducing the increase in calcium in the cells.

Cell signaling pathways mediating constriction of VSMCs

APJ, the endogenous receptor of apelin, has been reported to mediate apelin-induced cell effects (11), such as increasing the diameters of angiotensin II preconstricted efferent and afferent arterioles in the glomeruli (9). To prove the hypothesis that APJ expression is decreased in ECs and VSMCs of diabetic mice, cells were treated with high glucose. The results indicate that high glucose significantly decreased APJ expression in ECs and VSMCs (**Fig. 8*A–C***). These results suggest that inhibition of vascular tone by high glucose is associated with APJ expression.

NO is essential for vascular tone, and therefore apelin may impair myogenic tone in DN by increasing NO production in endothelial cells. The effects of apelin on eNOS were detected in endothelial cells after stretch inducement. The results indicate that stretch triggered a 30% decrease in eNOS phosphorylation, whereas this decrease was significantly eliminated by apelin and high glucose (Fig. 8*A, D*).

β-Arrestin is a bias signaling pathway for GPCRs, which is reported to mediate myogenic signaling in myocardium initiated by APJ (7, 11). To show that apelin inhibits stretch-induced VSMC contraction through inhibiting β-arrestin, the effects of apelin and stretch on β-arrestin in VSMCs were measured. A mechanical means of stretching was used. Stretching triggered a 185% enhancement of β-arrestin expression, but the increase was almost totally eliminated by apelin and high glucose (Fig. 8*A, E*).

Down-regulation of β-arrestin inhibited phosphorylation of MLC induced by stretching

To confirm that apelin inhibits phosphorylation of MLC through reducing expression of β-arrestin, Arrestin-C CRISPR was used to knock down the expression of β-arrestin. The results showed that the Arrestin-C CRISPR inhibited phosphorylation of MLC

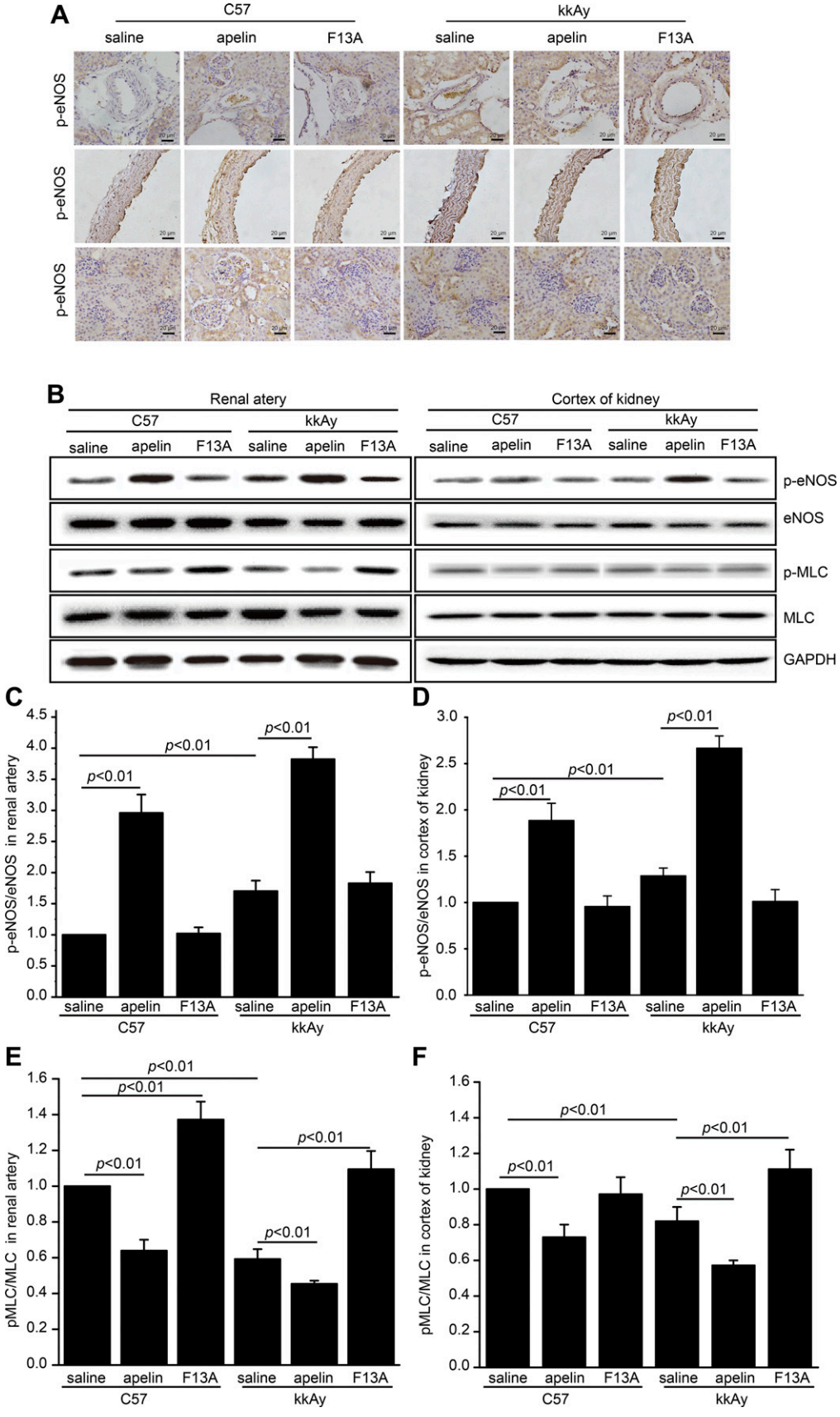

Figure 3. The effects of apelin on phosphorylation of eNOS and MLC. *A*) Representative images for immune staining of p-eNOS in renal artery and kidney cortex. *B*) Representative Western blots of eNOS and MLC. Apelin increased phosphorylation of eNOS in renal artery (*C*) and kidney cortex (*D*), whereas F13A did not show such effects. *E*) Apelin decreased phosphorylation of MLC in renal artery, whereas F13A increased it. *F*) Apelin decreased phosphorylation of MLC in kidney cortex, whereas F13A increased it ($n = 3$).

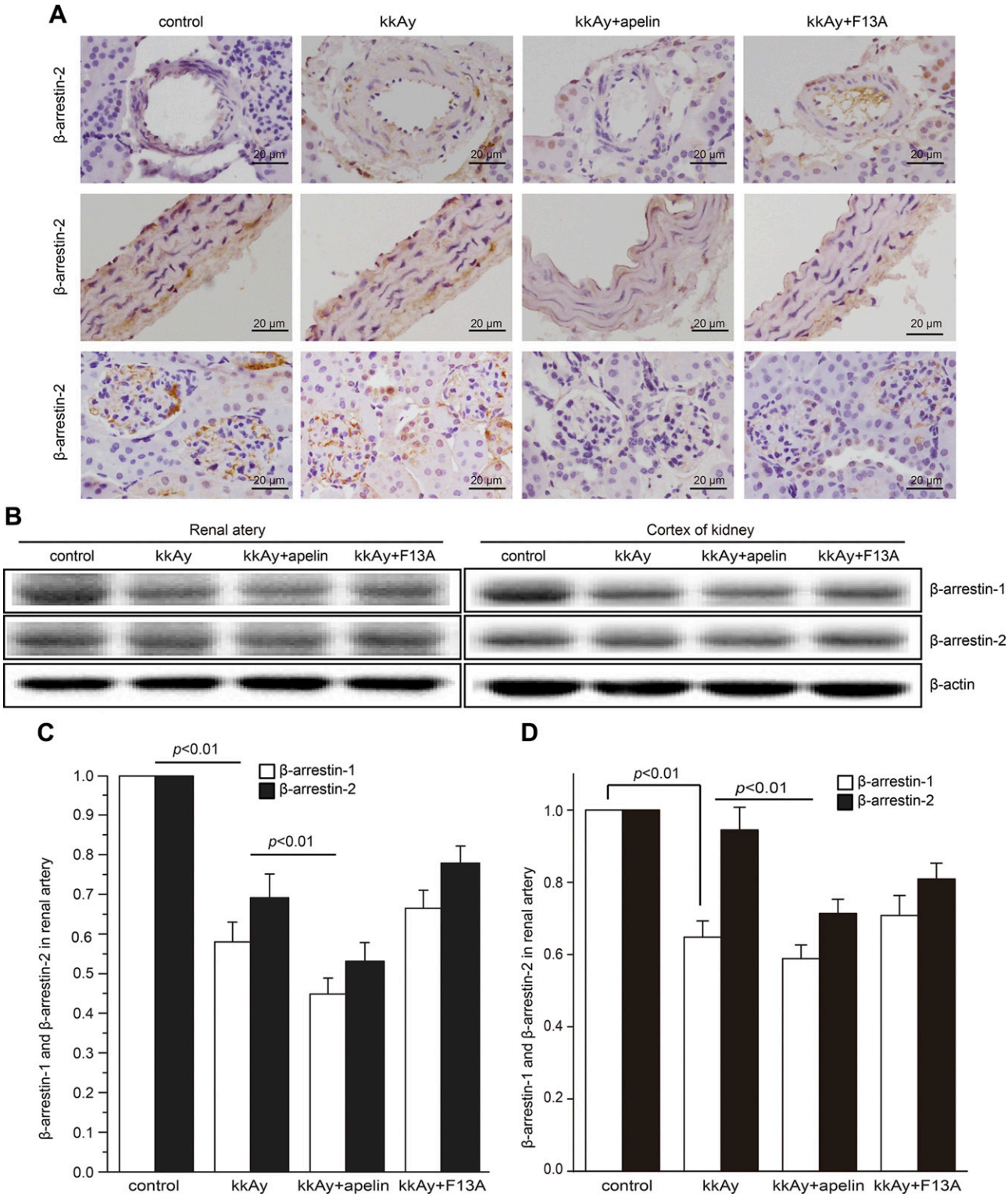

Figure 4. The effects of apelin on β-arrestin in renal artery and kidney cortex. *A*) Representative images of immune staining of β-arrestin in renal artery and kidney cortex. *B*) Representative Western blots of β-arrestin-1 and -2 in tissues. *C*) Relative expression of β-arrestin-1 and -2 in renal artery. Both β-arrestin-1 and -2 were decreased in kkAy mice, and apelin further decreased β-arrestin-1 and -2 expression in kkAy mice. *D*) Relative expression of β-arrestin-1 and -2 in renal artery. β-Arrestin-1 was decreased in kkAy mice, apelin decreased both β-arrestin-1 and -2 expression in kkAy mice ($n = 3$).

in VSMCs. Meanwhile, the inhibition of apelin on phosphorylation of MLC in VSMCs vanished after Arrestin-C CRISPR treatment VSMCs induced by stretching (**Fig. 9**).

DISCUSSION

RBF in diabetes mellitus has been reported be disturbed, which may lead to renal dysfunction (4, 20, 22,

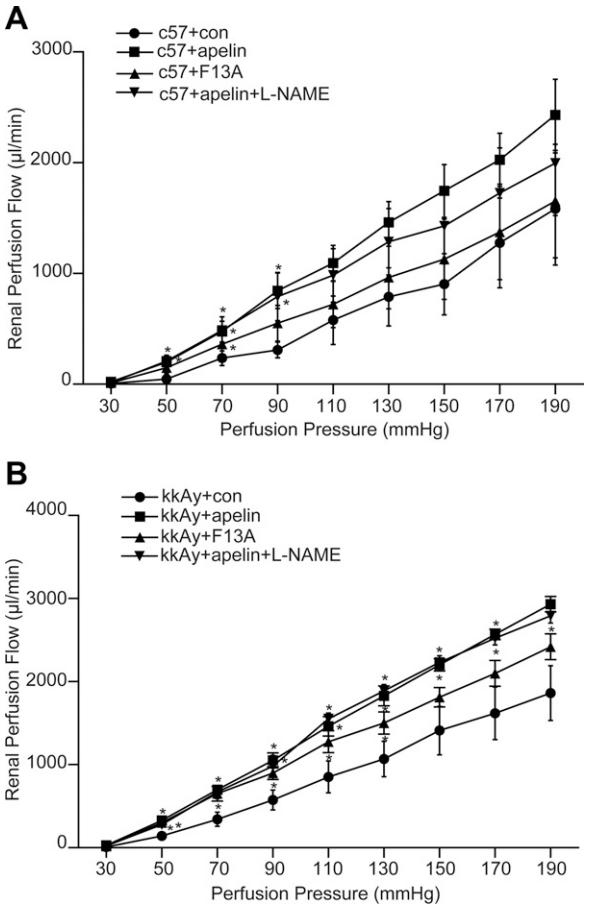

Figure 5. Relationships between pressure and flow in isolated perfused kidneys at 30–190 mmHg perfusion pressure. *A*) The pressure–flow relationship in isolated perfused kidneys from C57/BL mice. Apelin increased the perfusion flow, which was partially inhibited by L-NAME. The effects of F13A on increasing perfusion flow were less than that of apelin ($n = 6$). *$P < 0.05$ *vs.* kidneys from C57/BL mice. *B*) The pressure–flow relationship in isolated perfused kidneys from kkAy mice. Apelin increased the perfusion flow, which was not inhibited by L-NAME. The effect of F13A on increasing perfusion flow was less than that of apelin ($n = 6$). *$P < 0.05$ *vs.* kidneys from kkAy mice.

23). In the present study, the results showed for the first time that increased apelin in serum correlates positively with increased RBF and increases ACR in C57 and diabetic (kkAy) mice (Figs. 1 and 2). These results are consistent with previous reports that apelin promotes renal dysfunction in DN (3). However, the mechanisms for apelin-increased RBF are not fully understood.

In the present study, body weight and fasting blood glucose were not affected by apelin, whereas blood pressure was decreased by apelin in both control and diabetic mice (as shown in Tables 1 and 2). These results were consistent with those in previous studies, which found that apelin decreases blood pressure by dilating blood vessels (24), suggesting that apelin regulates RBF through dilating blood vessels in diabetic mice because of the increased concentration of apelin in serum (Fig. 1*D*). However, the results of blood glucose seemed discrepant with previous research (3, 25, 26), which may be related to the model of early-stage diabetes used in this study. Unfed kkAy 8-wk-old mice showed a minor increase in blood glucose, which suggests that insulin resistance in these mice may not be the same as in the late stage of diabetes mellitus. Therefore, the effects and mechanisms of apelin on blood glucose in diabetes mellitus should be investigated further.

NO has been shown to be a key pathway in controlling vascular tone and RBF (27, 28), whereas apelin has been reported to be involved in regulating vascular tone depending on the NO pathway (29) and to promote the progression of DN through endothelial cells (3) and podocyte injuries (30). In the present study, the results showed that p-eNOS was increased when accompanied with increased apelin in serum, both in the renal artery and kidney cortex (Fig. 3), which suggests that apelin dilates blood vessels in diabetic mice through increasing NO production.

Besides NO-dependent dilation, the myogenic response of VSMCs is important for controlling RBF (2). A rise in arterial pressure not only increases the force pushing blood through the vessels but also activates the myogenic mechanisms, reducing the vascular diameter to decrease the RBF. It is assumed that phosphorylation of MLC is essential for VSMC contraction in response to stretch stimuli (6). The results indicate that apelin decreased phosphorylation of MLC in the renal artery in C57 and kkAy mice. On the other hand, F13A, an antagonist of apelin, increased phosphorylation of MLC in the renal artery (Fig. 3). These results suggested that increased apelin in diabetic mice contributed to increased RBF in diabetic mice, which may be related to the impaired myogenic mechanisms induced by apelin in diabetic mice.

To investigate the direct effects of apelin on myogenic response of the renal arterioles, renal perfusion flow was measured in isolated perfused kidney at perfusion pressure of 30–190 mmHg. The results showed increased renal perfusion flow in kidneys of diabetic mice (kkAy) compared with kidneys from C57 mice (Fig. 5). Because no apelin was present in the perfusion fluid, these results suggest that decreased APJ in blood vessels, which can be induced by high glucose (Fig. 8), may also contribute to the impaired myogenic tone in diabetic mice. Apelin increased the perfusion flow of isolated kidneys from kkAy and C57 mice, which was partially inhibited by L-NAME in C57 mice. These results suggest that apelin impairs the myogenic response in kidney, an effect that is partially mediated by eNOS. F13A increased the perfusion flow of isolated kidneys from kkAy and C57 mice, as well, even though the increasing effects of F13A on perfusion flow were less than apelin. These results indicate that F13A may combine with APJ on the cells to compete with stretch stimulation, but no other activating effects of APJ would be exerted, such as eNOS, to relax blood vessels. What then may be the mechanism for apelin to impair myogenic tone?

Apelin has been reported to compete with stretching to attenuate transverse aortic constriction–induced

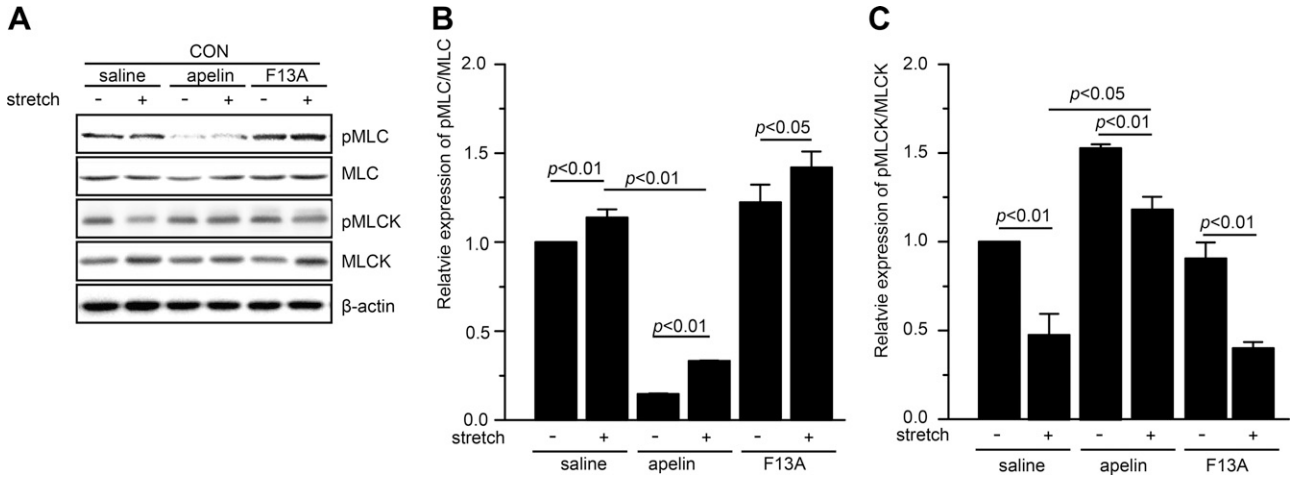

Figure 6. Stretch-induced contraction of VSMCs. *A*) Representative Western blots of MLC and MLCK in VSMCs. *B*) Relative expression of p-MLC/MLC. Stretch increased phosphorylation of MLC, apelin inhibited the phosphorylation of MLC, both in control and high-glucose conditions. *C*) Relative expression of p-MLCK/MLCK. Stretching increased and apelin inhibited the phosphorylation of MLCK in control and high-glucose conditions ($n = 3$).

cardiac hypertrophy (11), which is mediated by inhibiting β-arrestin signaling pathway. Is β-arrestin expression also mediated myogenic response of VSMCs? And what effects would apelin have on β-arrestin in VSMCs? The results in the present study showed that β-arrestin-1 and -2 were both decreased in kkAy mice and were further decreased by apelin, but increased by F13A (Fig. 4). These results suggest that apelin impairs the myogenic response of VSMCs in DN through decreasing β-arrestin.

To verify the effects of apelin on the myogenic response in VSMCs, we applied mechanical stretching. The results show that phosphorylation of MLC in VSMCs was increased by stretching, whereas phosphorylation of MLCK in VSMCs was decreased by it. Apelin decreased phosphorylation of MLC and increased phosphorylation of MLCK in VSMCs induced by stretching, whereas F13A did not show such effects. These results suggest that apelin impairs myogenic response in VSMCs by inhibiting cell contraction. However, it is reported that apelin stimulates MLC phosphorylation in VSMCs (31), which seems to contradict the present results. This difference may be related to the different concentrations used for the stimulation and the duration of the stimulation: apelin stimulates phosphorylation of MLC in VSMCs in a time- and concentration-dependent pattern (31). The concentration used in this study (1.0 nM) was the lowest used in the previous study, because the physiologic and pathologic concentrations (3) are close to that level. The stimulation time (30 min) in this study was longer than that in the previous study, because the pathologically increased apelin would be applied on the cell continuously. Therefore, it could be proposed that lengthy exposure of apelin (at pathological concentration) to VSMCs would inhibit cell contraction.

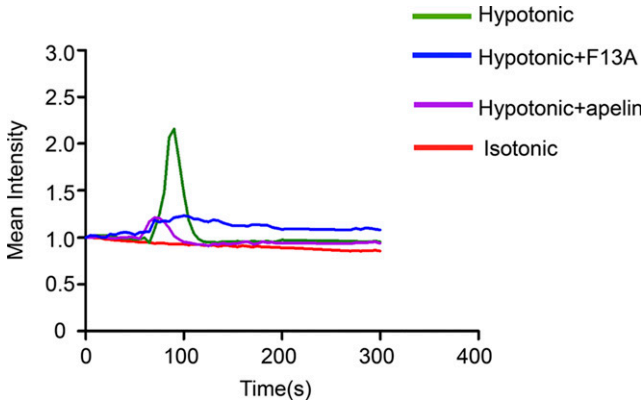

Figure 7. Calcium change in VSMCs. VSMCs precultured with Fluo-4 AM were treated with isotonic or hypotonic HEPES buffer; and the fluorescence indicating the calcium concentration was detected with a confocal microscope. Both apelin and F13A decreased the hypotonic HEPES buffer–induced increase in calcium concentration in VSMCs ($n = 3$).

Calcium has been reported to be necessary for cell contraction, and the results in this study indicate that both apelin and F13A inhibited the increase of calcium in VSMCs induced by hypotonic stretching. These results suggested that apelin competed with stretching to attenuate the stretch-induced cell contraction. F13A possesses an amino acid sequence and structure similar to that of apelin and may combine with the receptor APJ to compete with stretch stimulation, but without activation of G protein. When F13A was exposed to cultured smooth muscle cells where no apelin was present in the medium, it acted as a competitive factor to reduce the response of APJ to stretching, which resulted in reduced calcium just as apelin did on stretch-stimulated VSMCs. However, when F13A was applied to mice whose serum contains apelin, it competed with apelin to combine with APJ on the endothelial cells, which reduced the production of eNOS and relaxation of blood vessels.

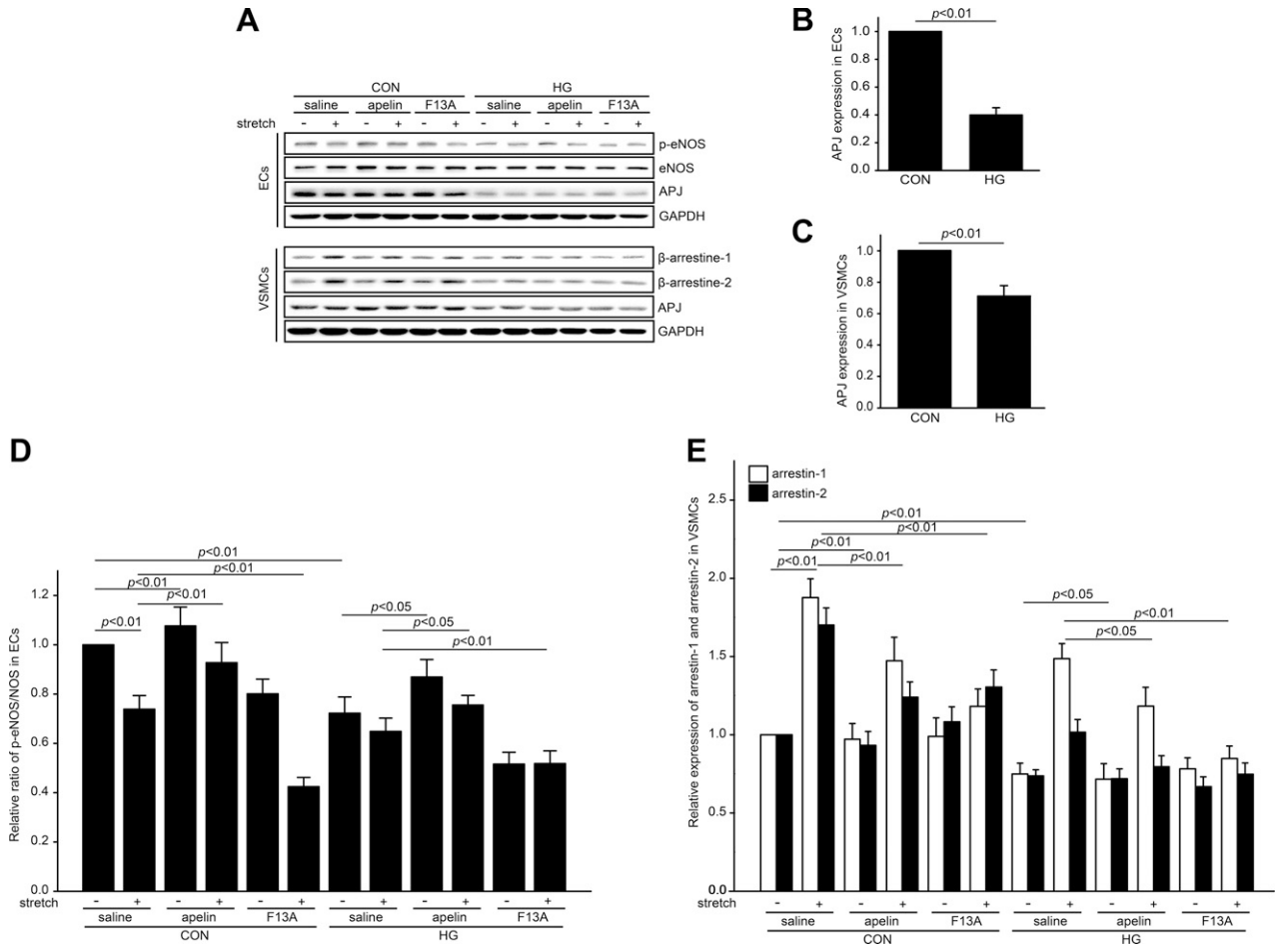

Figure 8. High glucose decreased APJ expression both in ECs and VSMCs. Stretch-induced phosphorylation of eNOS in ECs and increased expression of β-arrestin-1 and -2 in VSMCs (n = 3). *A*) Representative Western blots of p-eNOS, eNOS, APJ, and β-arrestin-1 and 2. *B*) High glucose decreased APJ expression in ECs. *C*) High glucose decreased APJ expression in VSMCs. *D*) Stretching inhibited the phosphorylation of eNOS in ECs, high glucose decreased the stretch-induced inhibition of p-eNOS, apelin increased the phosphorylation of eNOS, and F13A decreased the phosphorylation of eNOS in ECs. *E*) Stretching increased β-arrestin-1 and -2 expression in VSMCs, high glucose decreased the expression of β-arrestin-1 and -2 in VSMCs, apelin inhibited the increase in of β-arrestin-2 induced by stretching, and F13A inhibited the increase in both β-arrestin-1 and -2 induced in VSMCs by stretching.

It has been reported that apelin competes with stretching to inhibit the β-arrestin pathway by combining with the receptor APJ (11). The results in the present study showed that high glucose decreased APJ expression in ECs and VSMCs. p-eNOS in ECs and β-arrestin in VSMCs were decreased, as well. These results indicate that stretching induced a decrease in p-eNOS in ECs, and an increase in β-arrestin in VSMCs may be mediated by the receptor APJ. Mechanical stretching triggered enhancement of β-arrestin expression in VSMCs, whereas apelin and high glucose reversed this increase in VSMCs. These results suggest that apelin inhibits stretch-induced VSMC contraction by decreasing β-arrestin through combing with APJ.

To show that β-arrestin mediates the myogenic response of VSMCs, β-arrestin CRISPR/Cas9 KO plasmids were used to knock down the expression of β-arrestin in VSMCs. The results showed that stretch-induced phosphorylation of MLC was inhibited after β-arrestin knockdown, and apelin showed no inhibition of p-MLC induced by stretching after β-arrestin knock down. These results confirm that apelin impairs the myogenic response in VSMCs by inhibiting the β-arrestin pathway.

Besides combining with APJ on VSMCs, apelin could combine with APJ on ECs to dilate blood vessels by releasing NO (10). The results in Fig. 8*A, D* showed that stretching decreased p-eNOS in ECs and that the effect was reversed by apelin. These results suggest that apelin impairs myogenic vasoconstriction by inducing NO release from ECs.

CONCLUSIONS

Mechanical response of VSMCs is necessary to trigger myogenic contraction in blood vessels. Apelin does not induce a myogenic response, but blunts the stretch- or blood pressure change–induced VSMC contraction through the eNOS and β-arrestin pathway,

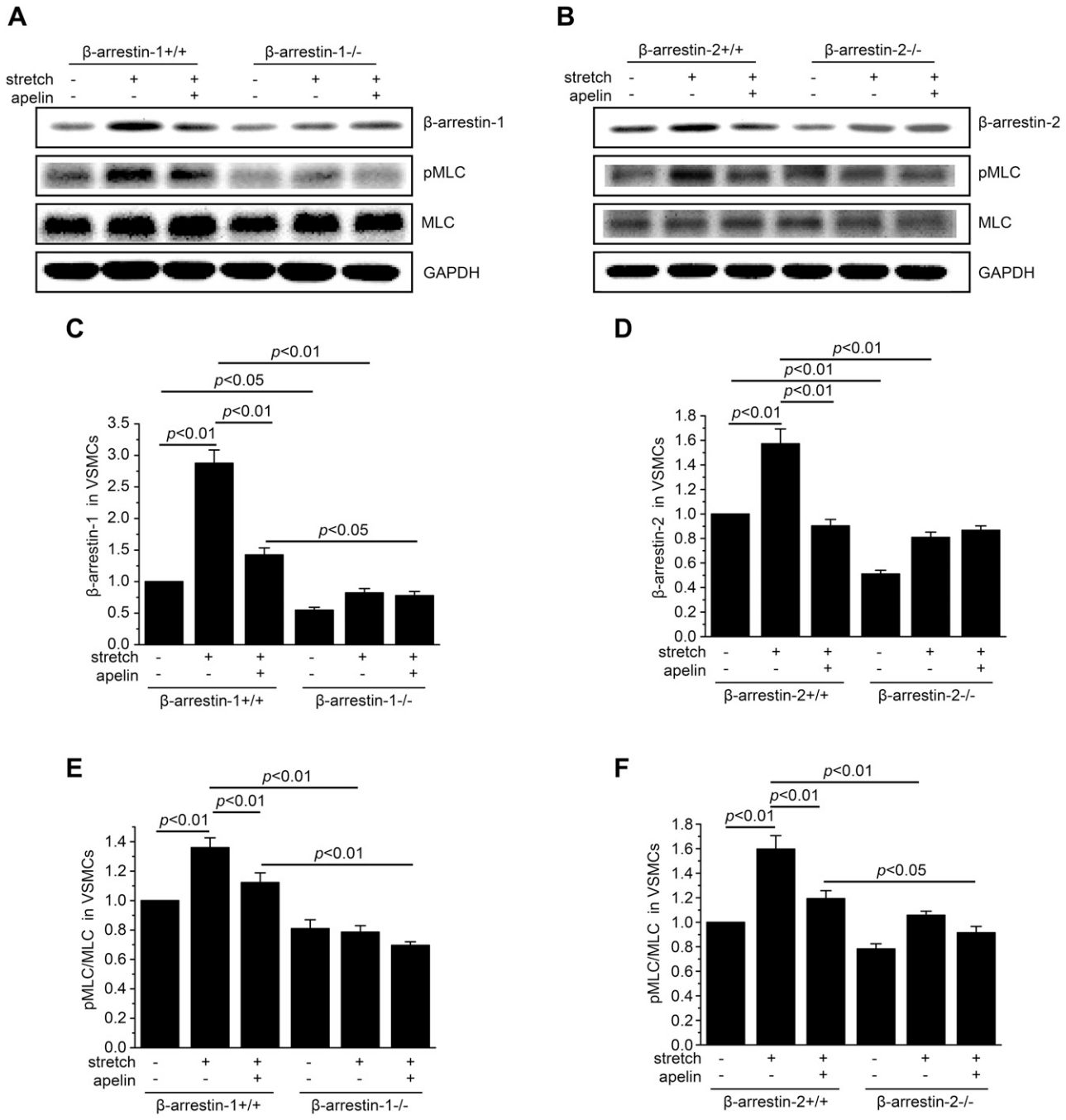

Figure 9. Effects of β-arrestin knockdown on phosphorylation of MLC in VSMCs ($n = 3$). Representative Western blots for p-MLC, MLC, β-arrestin-1 (*A*), and β-arrestin-2 (*B*). β-arrestin-1 (*C*) and β-arrestin-2 (*D*) were down-regulated by the CRISPR/Cas9 KO plasmid. *E*, *F*) Stretch-induced phosphorylation of MLC in VSMCs.

which suggests the ability of apelin to override physiologic signaling in myogenic response of blood vessels. At the cell signaling level, apelin may counteract myogenic response by inducing phosphorylation of eNOS in ECs and inhibit stretch-induced β-arrestin expression in VSMCs through combination with APJ.

Because of the animal models used in this study, the results may be discrepant in other diabetic animals. Therefore, this study should be repeated on different animal models before it is developed into a treatment for DN. The correlation between apelin and RBF was shown in patients with diabetes, and therefore, F13A or other antagonists of apelin could be used as a drug to prevent the progression of DN in patients.

ACKNOWLEDGMENTS

The authors thank Wei Wang, Haixia Huang, and Sitao Zhang (Capital Medical University) for assistance with the *ex vivo* study. The work was supported by the Natural Science Foundation of China Grant 81270815. The authors declare no conflicts of interest.

AUTHOR CONTRIBUTIONS

X. Zeng designed the study; J. Zhang analyzed the data; J. hang, Y. Wang, and B. Li performed the experiments; J. Yin and X. Zeng gave suggestions for the study and critically revised the manuscript; J. Zhang and J. Yin wrote the manuscript; and X. Zeng got the funding.

REFERENCES

1. Loutzenhiser, R., Bidani, A., and Chilton, L. (2002) Renal myogenic response: kinetic attributes and physiological role. *Circ. Res.* **90**, 1316–1324
2. Carlström, M., Wilcox, C. S., and Arendshorst, W. J. (2015) Renal autoregulation in health and disease. *Physiol. Rev.* **95**, 405–511
3. Zhang, B. H., Wang, W., Wang, H., Yin, J., and Zeng, X. J. (2013) Promoting effects of the adipokine, apelin, on diabetic nephropathy. *PLoS One* **8**, e60457
4. Schofield, I., Malik, R., Izzard, A., Austin, C., and Heagerty, A. (2002) Vascular structural and functional changes in type 2 diabetes mellitus: evidence for the roles of abnormal myogenic responsiveness and dyslipidemia. *Circulation* **106**, 3037–3043
5. Khavandi, K., Greenstein, A. S., Sonoyama, K., Withers, S., Price, A., Malik, R. A., and Heagerty, A. M. (2009) Myogenic tone and small artery remodelling: insight into diabetic nephropathy. *Nephrol. Dial. Transplant.* **24**, 361–369
6. Kauffenstein, G., Laher, I., Matrougui, K., Guérineau, N. C., and Henrion, D. (2012) Emerging role of G protein-coupled receptors in microvascular myogenic tone. *Cardiovasc. Res.* **95**, 223–232
7. Mederos y Schnitzler, M., Storch, U., Meibers, S., Nurwakagari, P., Breit, A., Essin, K., Gollasch, M., and Gudermann, T. (2008) Gq-coupled receptors as mechanosensors mediating myogenic vasoconstriction. *EMBO J.* **27**, 3092–3103
8. Kleinz, M. J., Skepper, J. N., and Davenport, A. P. (2005) Immunocytochemical localisation of the apelin receptor, APJ, to human cardiomyocytes, vascular smooth muscle and endothelial cells. *Regul. Pept.* **126**, 233–240
9. Hus-Citharel, A., Bouby, N., Frugière, A., Bodineau, L., Gasc, J. M., and Llorens-Cortes, C. (2008) Effect of apelin on glomerular hemodynamic function in the rat kidney. *Kidney Int.* **74**, 486–494
10. Zhong, J. C., Huang, Y., Yung, L. M., Lau, C. W., Leung, F. P., Wong, W. T., Lin, S. G., and Yu, X. Y. (2007) The novel peptide apelin regulates intrarenal artery tone in diabetic mice. *Regul. Pept.* **144**, 109–114
11. Scimia, M. C., Hurtado, C., Ray, S., Metzler, S., Wei, K., Wang, J., Woods, C. E., Purcell, N. H., Catalucci, D., Akasaka, T., Bueno, O. F., Vlasuk, G. P., Kaliman, P., Bodmer, R., Smith, L. H., Ashley, E., Mercola, M., Brown, J. H., and Ruiz-Lozano, P. (2012) APJ acts as a dual receptor in cardiac hypertrophy. *Nature* **488**, 394–398
12. Davis, M. J., and Hill, M. A. (1999) Signaling mechanisms underlying the vascular myogenic response. *Physiol. Rev.* **79**, 387–423
13. Murphy, T. V., Spurrell, B. E., and Hill, M. A. (2002) Cellular signalling in arteriolar myogenic constriction: involvement of tyrosine phosphorylation pathways. *Clin. Exp. Pharmacol. Physiol.* **29**, 612–619
14. Pierce, K. L., Premont, R. T., and Lefkowitz, R. J. (2002) Seven-transmembrane receptors. *Nat. Rev. Mol. Cell Biol.* **3**, 639–650
15. Tomino, Y. (2012) Lessons from the KK-Ay mouse, a spontaneous animal model for the treatment of human type 2 diabetic nephropathy. *Nephrourol. Mon.* **4**, 524–529
16. O'Brien, S. P., Smith, M., Ling, H., Phillips, L., Weber, W., Lydon, J., Maloney, C., Ledbetter, S., Arbeeny, C., and Wawersik, S. (2013) Glomerulopathy in the KK.Cg-A(y)/J mouse reflects the pathology of diabetic nephropathy. *J. Diabetes Res.* **2013**, 498925
17. Czogalla, J., Schweda, F., and Loffing, J. (2016) The mouse isolated perfused kidney technique. *J. Vis. Exp.* (117)
18. Wang, L., Zhao, X. C., Cui, W., Ma, Y. Q., Ren, H. L., Zhou, X., Fassett, J., Yang, Y. Z., Chen, Y., Xia, Y. L., Du, J., and Li, H. H. (2016) Genetic and pharmacologic inhibition of the chemokine receptor CXCR2 prevents experimental hypertension and vascular dysfunction. *Circulation* **134**, 1353–1368
19. Furgeson, S. B., Simpson, P. A., Park, I., Vanputten, V., Horita, H., Kontos, C. D., Nemenoff, R. A., and Weiser-Evans, M. C. (2010) Inactivation of the tumour suppressor, PTEN, in smooth muscle promotes a pro-inflammatory phenotype and enhances neointima formation. *Cardiovasc. Res.* **86**, 274–282
20. Seo, K. W., Lee, S. J., Ye, B. H., Kim, Y. W., Bae, S. S., and Kim, C. D. (2015) Mechanical stretch enhances the expression and activity of osteopontin and MMP-2 via the Akt1/AP-1 pathways in VSMC. *J. Mol. Cell. Cardiol.* **85**, 13–24
21. Zeng, X. J., Yu, S. P., Zhang, L., and Wei, L. (2010) Neuroprotective effect of the endogenous neural peptide apelin in cultured mouse cortical neurons. *Exp. Cell Res.* **316**, 1773–1783
22. Somlyo, A. P., and Somlyo, A. V. (2003) Ca2+ sensitivity of smooth muscle and nonmuscle myosin II: modulated by G proteins, kinases, and myosin phosphatase. *Physiol. Rev.* **83**, 1325–1358
23. Pihl, L., Persson, P., Fasching, A., Hansell, P., DiBona, G. F., and Palm, F. (2012) Insulin induces the correlation between renal blood flow and glomerular filtration rate in diabetes: implications for mechanisms causing hyperfiltration. *Am. J. Physiol. Regul. Integr. Comp. Physiol.* **303**, R39–R47
24. Maguire, J. J., Kleinz, M. J., Pitkin, S. L., and Davenport, A. P. (2009) [Pyr1]apelin-13 identified as the predominant apelin isoform in the human heart: vasoactive mechanisms and inotropic action in disease. *Hypertension* **54**, 598–604
25. O'Harte, F. P. M., Parthsarathy, V., Hogg, C., and Flatt, P. R. (2017) Acylated apelin-13 amide analogues exhibit enzyme resistance and prolonged insulin releasing, glucose lowering and anorexic properties. *Biochem. Pharmacol.* **146**, 165–173
26. Habchi, M., Duvillard, L., Cottet, V., Brindisi, M. C., Bouillet, B., Beacco, M., Crevisy, E., Buffier, P., Baillot-Rudoni, S., Verges, B., and Petit, J. M. (2014) Circulating apelin is increased in patients with type 1 or type 2 diabetes and is associated with better glycaemic control. *Clin. Endocrinol. (Oxf.)* **81**, 696–701
27. Jensen, E. P., Poulsen, S. S., Kissow, H., Holstein-Rathlou, N. H., Deacon, C. F., Jensen, B. L., Holst, J. J., and Sorensen, C. M. (2015) Activation of GLP-1 receptors on vascular smooth muscle cells reduces the autoregulatory response in afferent arterioles and increases renal blood flow. *Am. J. Physiol. Renal Physiol.* **308**, F867–F877
28. Dautzenberg, M., Keilhoff, G., and Just, A. (2011) Modulation of the myogenic response in renal blood flow autoregulation by NO depends on endothelial nitric oxide synthase (eNOS), but not neuronal or inducible NOS. *J. Physiol.* **589**, 4731–4744
29. Zhong, J. C., Yu, X. Y., Huang, Y., Yung, L. M., Lau, C. W., and Lin, S. G. (2007) Apelin modulates aortic vascular tone via endothelial nitric oxide synthase phosphorylation pathway in diabetic mice. *Cardiovasc. Res.* **74**, 388–395
30. Guo, C., Liu, Y., Zhao, W., Wei, S., Zhang, X., Wang, W., and Zeng, X. (2015) Apelin promotes diabetic nephropathy by inducing podocyte dysfunction via inhibiting proteasome activities. *J. Cell. Mol. Med.* **19**, 2273–2285
31. Hashimoto, T., Kihara, M., Ishida, J., Imai, N., Yoshida, S., Toya, Y., Fukamizu, A., Kitamura, H., and Umemura, S. (2006) Apelin stimulates myosin light chain phosphorylation in vascular smooth muscle cells. *Arterioscler. Thromb. Vasc. Biol.* **26**, 1267–1272

Received for publication November 5, 2017.
Accepted for publication February 26, 2018.